Neutron pickup from ^{33}S

D. J. Crozier,* A. Spadafora,† and H. T. Fortune
Physics Department, University of Pennsylvania, Philadelphia, Pennsylvania 19104
(Received 9 April 1979)

At a bombarding energy of 15 MeV, angular distributions have been measured for the $^{33}S(^3He,\alpha)$ reaction leading to 25 levels of ^{32}S below 8 MeV excitation. A distorted-wave Born approximation analysis has provided l values and relative spectroscopic factors for most of these. Results are in moderate agreement with shell-model calculations, but exhibit less configuration mixing than is predicted.

[NUCLEAR REACTIONS $^{33}S(^3He,\alpha)$, $E=15$ MeV, measured $\sigma(E_\alpha,\theta)$, enriched target; DWBA analysis, deduced l, π, J; comparison with shell model.]

I. INTRODUCTION

Little information is available concerning neutron pickup leading to ^{32}S. The latest compilation[1] lists only results for the first three states from a study[2] of $^{33}S(^3He,\alpha)$ at 10 MeV. A preliminary report of the reaction $^{33}S(p,d)$ has appeared,[3] but those results have not been published. We report here on an investigation of the $^{33}S(^3He,\alpha)$ reaction for states of ^{32}S below 8-MeV excitation.

Accurate excitation energies exist[1] for most levels below 8 MeV from studies of $^{31}P(^3He,d)$,[4] $^{34}S(p,t)$,[5] and from gamma decays following proton[6,7] and alpha[8] capture. In addition most of the levels now possess[1] unique J^π assignments.

II. EXPERIMENT

A 15-MeV ^3He beam bombarded a target of CdS that was enriched to 80% in ^{33}S. At the beginning

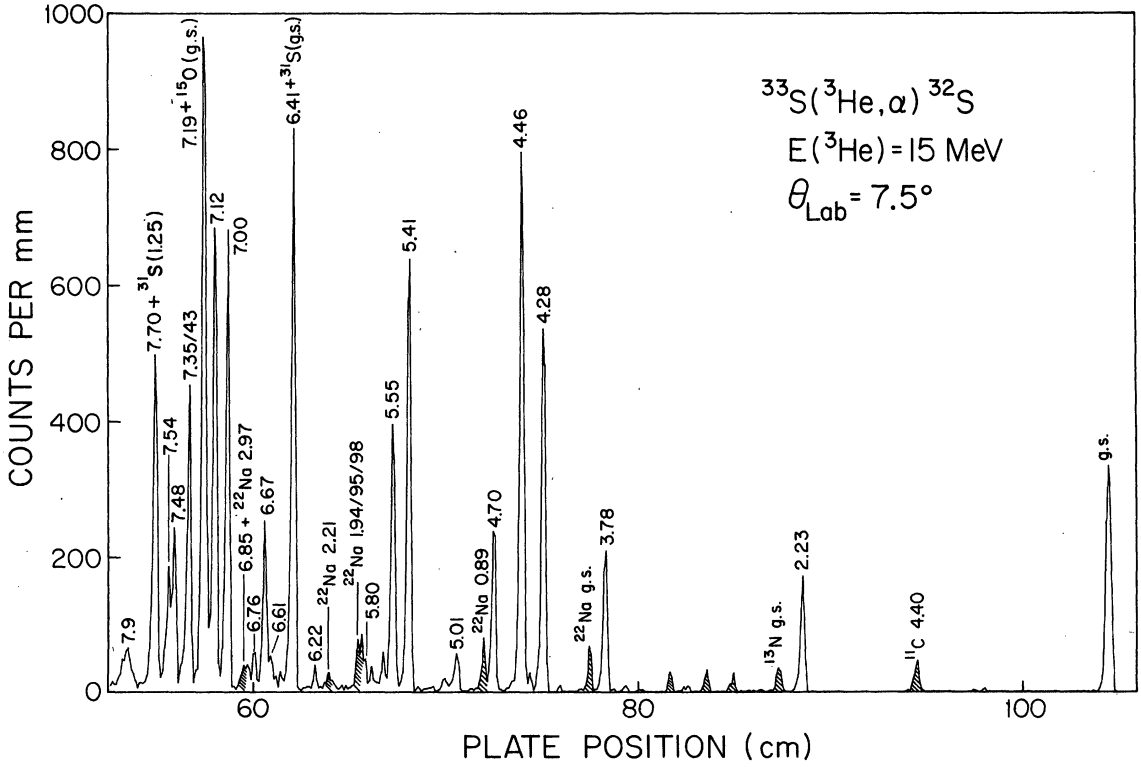

FIG. 1. Spectrum of the $^{33}S(^3He,\alpha)$ reaction.

of the experiment the target thickness was approximately 110 $\mu g/cm^2$ on a 5 $\mu g/cm^2$ Formvar backing. Outgoing alpha particles were momentum analyzed in a multiangle spectrograph and detected in nuclear emulsion plates. Data were collected in two separate exposures, each of which consisted of simultaneous collection of data at seven different angles, 7.5° apart, beginning at 3.75° and 7.5°. The two runs were normalized to one another by visual inspection of the angular distributions for low-lying states. Because the target evaporated during the run, absolute cross sections could not be reliably extracted. This target deterioration had no effect on the angular distributions since, for a given run, data were obtained at all angles simultaneously.

A spectrum is displayed in Fig. 1. Overall resolution is about 35 keV full width at half maximum (FWHM), and is determined primarily by target irregularities. Excitation energies were determined at each angle separately, using the observed peak positions and known magnet calibration. These energies were then averaged to obtain the values listed in Table I. In most cases, our results were in good agreement with values from the literature.[1]

Angular distributions are displayed in Figs. 2 and 3, where they are compared with distorted-wave Born approximation (DWBA) curves, to be discussed below. As mentioned earlier, absolute cross sections were not determined and hence the vertical scale is in arbitrary units. However, we expect that, to within a factor of 2, 1 arb. u = 1 mb/sr.

III. ANALYSIS

Theoretical angular distributions were computed with the code DWUCK,[9] using the optical-model parameters listed in Table II. These potentials gave

TABLE I. Excitation energies in ^{32}S.

Label	Excitation energy (keV) Present	(^{3}He, d) [a]	(p, d) [b]	Compilation [c]
g.s.	0.0	0	0	0
2.23	2232 ± 5	2229	2233	2230.3 ± 0.2
3.78	3781 ± 3	3778	3779	3778.3 ± 0.7
4.28	4284 ± 3	4280	4284	4281.5 ± 0.4
4.46	4462 ± 3	4463	4458	4458.9 ± 0.8
4.70	4698 ± 3	4695	4694	4695.4 ± 0.4
5.01	5010 ± 5	5006	5004	5006.2 ± 0.3
5.41	5409 ± 4	5415	5410	5413.0 ± 0.8
5.55	5547 ± 3	5550	5547	5548.9 ± 0.7
5.80	5796 ± 3	5802	5798	5797.9 ± 0.7
6.22	6226 ± 7	6222		6224.3 ± 0.7
6.41	6407 ± 5	6413		6411.0 ± 1.4
6.61	6612 ± 7	6580	(6581)	6581 ± 3
		6618	6621	6621.1 ± 0.3
6.67	6669 ± 4	6663	6666	6665.7 ± 0.8
6.76	6761 ± 4	6759	6762	6761.7 ± 0.3
6.85	6845 ± 12	6851	6852	6852 ± 2
7.00	6997 ± 4	7001	7002	7002.5 ± 1.0
7.12	7108 ± 7	7116	7116	7115.0 ± 1.2
7.19	7192 ± 6	7189	7191	7189.7 ± 1.2
7.35	7335 ± 7	7348	7351	7348 ± 2
7.43	7416 ± 11	7430		7434 ± 2
7.48	7481 ± 10	7485	7485	7484.8 ± 1.0
7.54	7538 ± 5	7538	7536	7535.7 ± 0.8
7.7	7648 ± 5	7701		7637 ± 5
				7701.7 ± 1.4
		7883		7886 ± 4
				7914 ± 5
7.9	7962 ± 17	7950		7950.1 ± 0.4
				7964 ± 3
		7973	7975	

[a] Reference 4. Uncertainty 5 keV.
[b] Reference 3 as quoted in Ref. 4.
[c] Reference 1.

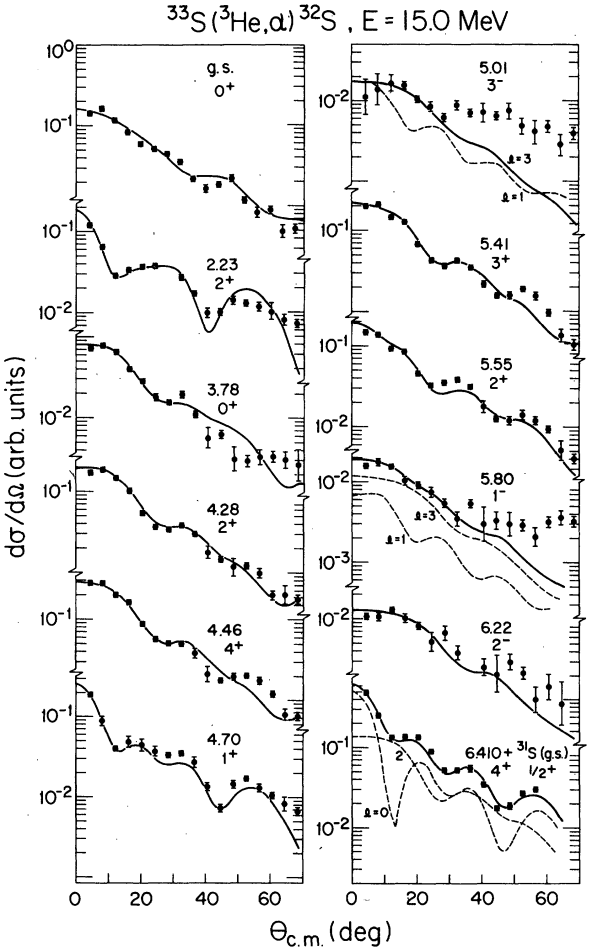

FIG. 2. Experimental angular distributions for the reaction $^{33}S(^3He, \alpha)^{32}S$, compared with DWBA curves.

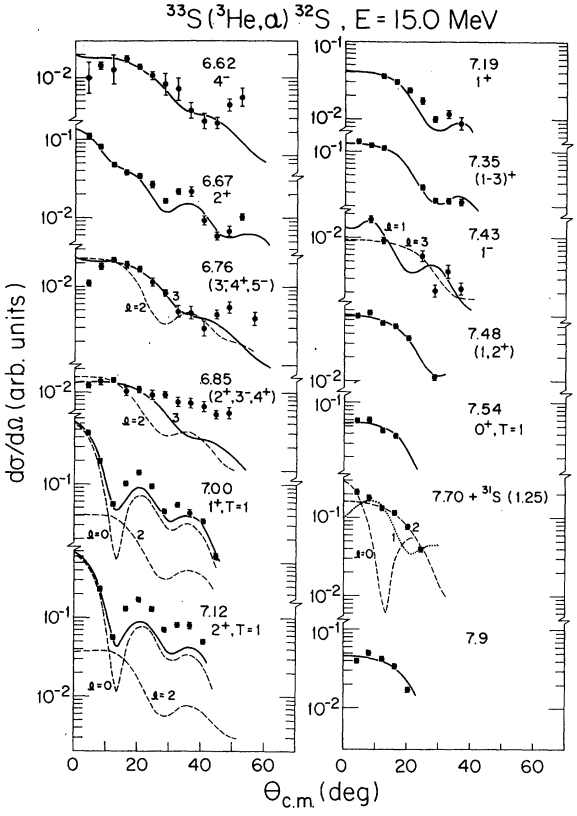

FIG. 3. Same as Fig. 1, but for higher excitation energy.

reasonable results in an earlier study[10] of ^{36}Ar-(^{3}He, α).

In the present experiment, virtually all of the strongly populated states have positive parity, as expected since the 1p-hole strength should be considerably higher than the cutoff of our experiment. States with $J^\pi = 1^+$ or 2^+ can be reached in ^{33}S-(^{3}He, α) via two l values, $l=0$ and/or 2, and for states with $J^\pi = 1^+ - 3^+$ the $l=2$ component can in principle contain both $1d_{3/2}$ and $1d_{5/2}$. Only 0^+-$(1d_{3/2})$ and $4^+(1d_{5/2})$ states are restricted by the selection rules to a single value of j (transferred total angular momentum).

The DWBA curves were normalized to the data,

TABLE II. Optical-model parameters used in analysis of ^{33}S(^{3}He, α)^{32}S. Potentials in MeV, lengths in fm.

	V	$r_0=r_{s0}$	$a=a_{s0}$	W	r_0'	a'	r_{0c}	V_{s0}
^{3}He	130	1.31	0.61	24	1.43	1.01	1.40	10
α	180	1.42	0.56	16.5	1.42	0.56	1.40	0
n	···	1.26	0.60	···	···	···	···	λ=25

with the aid of the expression

$$\sigma_{\exp}(\theta) = NC^2 \sum_{lj} S_{lj} \frac{\sigma_{lj}(\theta)}{2j+1},$$

where the sum is over the allowed l and j values discussed above. For 0^+ and 4^+ final states, the $l=2$ curves were calculated for $1d_{3/2}$ and $1d_{5/2}$ transfer, respectively. For states with $J^\pi = 1^+ - 3^+$, the $l=2$ curve for a given state was computed for the j value ($\frac{3}{2}$ or $\frac{5}{2}$) that is predicted by a recent shell-model calculation[11] to dominate for that state. For a fixed excitation energy, the theoretical angular distribution for $1d_{3/2}$ is only about one-half that for $1d_{5/2}$, so that for the same data, assumption of pure $1d_{3/2}$ yields a spectroscopic factor about 1.3 times that extracted assuming pure $1d_{5/2}$.

For mixed l transitions, the admixtures were varied to obtain the best fit to the angular distribution shapes. For a few cases, the decomposition is shown explicitly. Otherwise only the best fit curve is displayed.

The value of N for a (^{3}He, α) reaction is still not well known, so our lack of knowledge of an absolute cross section scale is not serious. Spectroscopic factors listed in Table III correspond to $N=10$ if 1 arb. u = 1 mb/sr. This is not very different from a recent value of $N=18$, obtained[12] by comparing (^{3}He, α) and (d, t) data.

For $T=0$ final states, the square of the isospin Clebsch-Gordan coefficient is unity, whereas for $T=1$ final states, we have $C^2=\frac{1}{2}$.

IV. RESULTS

In general, the angular-distribution shapes are well fitted. Slight exceptions are some of the negative-parity states (all of which are weakly populated) and the $l=0$ transitions at high E_x, where the DWBA curve underpredicts the second maximum.

Relative spectroscopic factors are listed in Table III, along with the nlj values used in the DWBA calculations. Also listed in Table III are the values of S predicted[11] by the shell-model calculation for the positive-parity states. Whenever both $1d_{5/2}$ and $1d_{3/2}$ can contribute, both are listed; the first number is for the nlj listed in column 3, the second is for the alternate possibility.

The most obvious conclusion that arises from comparing experimental and theoretical S value is that the shell model contains too much configuration mixing. The experimental S's for $1d_{5/2}$ transfer are consistently smaller than predicted, whereas for $1d_{3/2}$ the opposite is true. This is clearly seen in Table IV—the experimental $l=2$ spectroscopic factor sum for states predicted to

TABLE III. Spectroscopic factors for $^{33}S \rightarrow {}^{32}S + n$.

E_x	J^π	nlj	Spectroscopic factor Present	Shell model
0.0	0^+	$1d_{3/2}$	0.80	0.54
2.23	2^+	$1d_{5/2}$	0.068	0.048(0.009)
		$2s_{1/2}$	0.48	0.28
3.78	0^+	$1d_{3/2}$	0.16	0.082
4.28	2^+	$1d_{5/2}$	0.27	0.20(0.11)
		$2s_{1/2}$	~0	0.027
4.46	4^+	$1d_{5/2}$	0.36	0.50
4.70	1^+	$1d_{3/2}$	0.076	0.013(0.0009)
		$2s_{1/2}$	0.18	0.21
5.01	3^-	$1f_{7/2}$	0.015	...
5.41	3^+	$1d_{5/2}$	0.25	0.30(0.045)
5.55	2^+	$1d_{3/2}$	0.19	0.13(0.045)
		$2s_{1/2}$	0.032	0.038
5.80	1^-	$1f_{5/2}$	0.010	...
		$2p_{3/2}$	0.004	...
6.22	2^-	$1f_{7/2}$	0.016	...
6.41	4^+	$1d_{5/2}$	0.18	0.50
6.62	4^-	$1f_{7/2}$	0.025	...
6.66	2^+	$1d_{5/2}$	0.066	0.13(0.0009)
		$2s_{1/2}$	0.030	0.0005
6.76	$(3^-, 4^+, 5^-)$	$1f_{7/2}$	0.030	...
6.85	$(2^+, 3^-, 4^+)$	$1f_{7/2}$	0.018	...
		or $1d_{5/2}$	0.018	...
7.00	$1^+, T=1$	$1d_{3/2}$	0.19	0.11(0)
		$2s_{1/2}$	0.56	0.60
7.12	$2^+, T=1$	$1d_{5/2}$	0.14	0.056(0.002)
		$2s_{1/2}$	0.63	0.91
7.19	1^+	$1d_{5/2}$	0.048	0.21(0)
		$2s_{1/2}$	~0	0
7.35	$(1-3)^+$	$1d_{5/2}$	0.15	0.16 [a] (0.024)
7.43	1^-	$(2p_{3/2})$	0.007	...
7.48	$(1, 2^+)$	$1d_{5/2}$	0.078	...
7.54	$0^+, T=1$	$1d_{3/2}$	0.29	0.061
7.64		$1d_{5/2}$	0.19	...
7.70		or $2s_{1/2}$	0.06	...
		or $2p_{3/2}$	0.06	...
7.89		$1d_{5/2}$	0.05	...
7.91				

[a] 3^+ at 7.109.

TABLE IV. Comparison of spectroscopic factor sums for $T=0$ states.

nlj	Experimental	Shell model
$1d_{3/2}$	1.23	0.82
$1d_{5/2}$	1.24	2.05
$2s_{1/2}$	0.72	0.56
Sum	3.19	3.43

be populated dominantly by $1d_{3/2}$ is very nearly equal to that for $1d_{5/2}$, whereas the shell model predicts a preponderance of $1d_{5/2}$ to $1d_{3/2}$ by a factor of about 2.5. This feature is especially obvious for 0^+ and 4^+ states, which can be reached only via $1d_{3/2}$ and $1d_{5/2}$, respectively. For every 0^+ level the measured S is larger than that predicted, whereas for all 4^+ states the measured S values are smaller than the shell-model ones.

We turn now to a discussion of those states whose J^π assignments are still uncertain. The 6.76-MeV state has natural parity from (α, α') (Ref. 13) and $J=3$–5 from (p, γ) implying $J^\pi = 3^-$, 4^+, or 5^-. The $(^3\mathrm{He}, \alpha)$ cross section for this state is quite small, but its angular distribution is fitted much better by $l=3$ than by $l=2$, suggesting a strong preference for negative parity.

The 6.85-MeV level also has natural parity from (α, α'), but $J=2$–4 from γ decays. For this state, neither $l=2$ nor 3 fits the $(^3\mathrm{He}, \alpha)$ angular distribution, which is rather featureless. However, the lowest 2^+ and 4^+ shell-model states that do not have experimental counterparts are above 7.5 MeV. We thus favor 3^- for the 6.85-MeV state.

The 7.35-MeV state, which was assigned[4] $J^\pi = (1-3)^+$ in $^{31}\mathrm{P}(^3\mathrm{He}, d)$, has a clear $l=2$ angular distribution in the present work. A shell-model state with $J^\pi = 3^+$, at $E_x = 7.1$ MeV, remains to be located in the experimental spectrum. Both from its excitation energy and S_n, we favor identifying it with the 7.35-MeV experimental state.

Our $l=2$ angular distribution for the 7.48-MeV level established positive parity for it. We tentatively identify it with a 2^+ model state predicted at 7.51 MeV.

Our 7.7-MeV angular distribution contains contributions from ^{32}S states at 7.64 and 7.70 MeV, and from the $^{32}\mathrm{S}(^3\mathrm{He}, \alpha)$ reaction to the 1.25-MeV $\frac{3^+}{2}$ state of ^{31}S. It cannot be fitted by any single l value, but appears to consist of $l=0+2$. All of the $l=2$ component could arise from the ^{31}S state, but, of course, none of the $l=0$. This would suggest $J^\pi = 1^+$ or 2^+ for one of the two ^{32}S levels. The 7.64-MeV state has no previous J^π information. The 7.70-MeV level is listed in the latest compilation with $J^\pi = (1-4^+)$ from γ decay, whereas an $l=3$ assignment in $(^3\mathrm{He}, d)$ implies $J^\pi = (2-4)^-$. There may actually be three states here.

Our 7.9-MeV peak could encompass two known states at 7.886 and 7.914 MeV, the first of which has $J^\pi = (2-4)^-$ in the compilation and $J^\pi = (0-2)^-$ from $(^3\mathrm{He}, d)$. Our limited angular distribution is best fitted by $l=2$, perhaps implying that it mostly arises from the 7.91-MeV state and that this level has positive parity.

In conclusion, we favor negative parity for the states at 6.76 and 6.85 MeV and positive parity for states at 7.35, 7.48, 7.7, and 7.9 MeV. The 7.35-MeV level probably has $J^\pi = 3^+$ and the 7.48 MeV state 2^+. Somewhat of a puzzle is the location of

two 0^+ $T=0$ states predicted near 7.1 MeV, but not observed.

Comparison with shell-model calculations shows very good overall agreement in excitation energies and moderate agreement with spectroscopic factors. But the shell model predicts more configuration mixing among the low-lying states than is observed experimentally. Similar conclusions were reached in the recent ^{31}P(^{3}He, d) study.

We acknowledge financial support from the National Science Foundation. We are grateful to W. Chung and B. H. Wildenthal for providing their shell-model results prior to publication.

---

*Present address: Control Data Corporation, Southfield, Michigan 48075.

†Present address: Department of Physics, University of Illinois, Urbana, Ill. 61801.

[1]P. M. Endt and C. Van der Leun, Nucl. Phys. A310, 1 (1978).

[2]G. Inglima *et al.*, Nuovo Cimento 26A, 211 (1975).

[3]D. L. Show, A. S. Moalem, and B. H. Wildenthal, Bull. Am. Phys. Soc. 19, 74 (1974).

[4]J. Kalifa *et al.*, Phys. Rev. C 17, 1961 (1978).

[5]H. Nann and B. H. Wildenthal, Phys. Rev. C 13, 1009 (1976).

[6]J. Vernotte, S. Gates, M. Langevin, and J. M. Maison, Nucl. Phys. A212, 493 (1973).

[7]J. Vernotte *et al.*, Phys. Rev. C 13, 984 (1976).

[8]D. W. O. Rogers, W. R. Dixon, and R. S. Storey, Nucl. Phys. A281, 345 (1977).

[9]P. D. Kunz, private communication.

[10]R. R. Betts, H. T. Fortune, and R. Middleton, Phys. Rev. C 8, 660 (1973).

[11]W. Chung and B. H. Wildenthal, private communication.

[12]E. Friedman, A. Moalem, D. Suraqui, and S. Mordechai, Phys. Rev. C 15, 1604 (1977).

[13]P. R. Gardner *et al.*, Aust. J. Phys. 26, 747 (1973).

[14]H. Grawe, J. E. Cairns, M. W. Greene, and J. A. Kuehner, Can. J. Phys. 52, 950 (1974).